

Direct measurement of the Higgs self-coupling in $e^+e^- \rightarrow ZH$

Junya Nakamura*

Institut für Theoretische Physik, Universität Tübingen, 72076 Tübingen, Germany

Ambresh Shiva[†]

Centre for Cosmology, Particle Physics and Phenomenology (CP3),

Université Catholique de Louvain, B-1348 Louvain-la-Neuve, Belgium

Abstract

A new method to measure the trilinear Higgs self-coupling λ_3 in a single Higgs production process is proposed. Time-reversal-odd (T-odd) asymmetries in the process $e^+e^- \rightarrow ZH, Z \rightarrow f\bar{f}$ are computed from the absorptive part of the electroweak one-loop amplitude. Since the T-odd asymmetries measure the tree-level t -channel $ZH \rightarrow ZH$ scattering, they can be direct probes of λ_3 . The proposed method is quite challenging; a relatively large statistics and polarized e^+e^- beams are demanded. However, this is probably the only approach to directly measure λ_3 in e^+e^- collisions, when a beam energy above the ZHH production threshold is not available.

arXiv:1812.01576v1 [hep-ph] 4 Dec 2018

* junya.nakamura@itp.uni-tuebingen.de

† ambresh.shivaji@uclouvain.be

The capabilities of the LHC and future e^+e^- colliders to measure the trilinear Higgs self-coupling λ_3 have been extensively studied in recent years [1–26]. Unlike the couplings of the Higgs bosons with heavy fermions and gauge bosons, we do not have any meaningful information on λ_3 and its value can be very different from the one predicted in the standard model (SM). The measurements from the di-Higgs production processes, which are commonly referred as *direct* measurements, are challenging, because of their very small cross sections both at the LHC [1, 2, 4, 5, 9, 10, 15, 21] and at e^+e^- colliders [3, 6, 7, 17, 22], at which a relatively high beam energy is required. Current LHC runs are only able to provide exclusion limits for di-Higgs production [20, 24] and, even the projected sensitivity at the HL-LHC is very weak ($-0.8 < \lambda_3/\lambda_3^{\text{SM}} < 7.7$) [19, 26]. The information on λ_3 may be also obtained from measurement of the (differential) cross sections of the single Higgs production processes [8, 11–14, 16–18, 22, 23, 27]. The coupling λ_3 contributes to the electroweak one-loop correction to single Higgs processes. This approach is commonly called an *indirect* one due to the fact that the trilinear coupling enters into the loop. Since very precise determination of the cross sections is demanded, the indirect method in single Higgs processes is as challenging as the direct measurement from the di-Higgs productions [8, 16, 17, 22].

In e^+e^- collisions, the aforementioned indirect method in the process $e^+e^- \rightarrow ZH$ has an obvious advantage over the direct approach with the di-Higgs production processes such as $e^+e^- \rightarrow ZHH$; only a smaller beam energy is needed. However, the indirect measurements highly depend on assumptions about unknown new physics (NP) at high scale that does not modify the coupling λ_3 itself [8]¹. Direct methods, on the other hand, are less model dependent and, therefore, can provide more reliable bounds on a possible modification of λ_3 .

In this work, a method of measuring *directly* the coupling λ_3 in the single Higgs production process $e^+e^- \rightarrow ZH$ is proposed. The method deals with time-reversal-odd (T-odd) asymmetries in the production process with a subsequent Z boson decay into a massless fermion pair,

$$e^+e^- \rightarrow Z(\rightarrow f\bar{f}) + H. \quad (1)$$

When CP (or equally T) is conserved, T-odd quantities are generally identical to zero in the tree-level approximation and receive finite contributions only from an absorptive part

¹ It is known that a virtual heavy fermion in the one-loop radiative correction does not decouple from the cross section measured at low energy [28–31].

of loop diagrams [32]. The T-odd asymmetries are computed at the lowest order from the absorptive part of the electroweak one-loop amplitude. The absorptive part always includes the tree level t -channel $ZH \rightarrow ZH$ re-scattering effect, a part of which is proportional to the coupling λ_3 . As a result, the T-odd asymmetries are direct probes of λ_3 . Unknown heavy NP particles, which may affect the indirect λ_3 measurement via one-loop radiative corrections, do not contribute to the T-odd asymmetries unless the beam energy is large enough to directly produce these NP particles, because the asymmetries arise only from the absorptive part ².

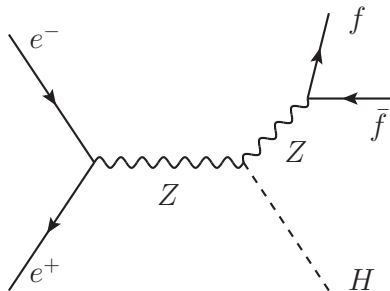


FIG. 1. Tree-level Feynman diagram for the process $e^+e^- \rightarrow Z(\rightarrow f\bar{f}) + H$.

The kinematics of the process in Eq. (1) can be specified by four independent variables after integration over the azimuthal angle of the Z : the center-of-mass (c.m.) energy squared s , the polar angle Θ ($0 \leq \Theta \leq \pi$) of the Z from the direction of the e^- momentum in the e^+e^- c.m. frame, the polar θ and azimuthal ϕ angles of the final fermion f in the Z rest frame. We neglect the initial electron mass and the final fermion mass. For given s and the electron helicity (τ), after the summation over the final fermion helicity, the differential cross section using the narrow width approximation for the Z boson can be expressed as ³

$$\begin{aligned} \frac{d^3\sigma(\tau)}{d\cos\Theta d\cos\theta d\phi} = & F_1(1 + \cos^2\theta) + F_2(1 - 3\cos^2\theta) + F_3\sin 2\theta\cos\phi + F_4\sin^2\theta\cos 2\phi \\ & + F_5\cos\theta + F_6\sin\theta\cos\phi + F_7\sin\theta\sin\phi + F_8\sin 2\theta\sin\phi + F_9\sin^2\theta\sin 2\phi, \end{aligned} \quad (2)$$

² It should be noted that the attempt to directly measure a coupling which enters a process at the next-to-leading order by using T-odd observables is not new in particle physics; see e.g. [33–37].

³ s dependence is always implicit throughout the paper.

where the nine coefficients F_i ($i = 1$ to 9) are functions of τ , s and $\cos \Theta$. After integrations over θ and ϕ , only F_1 remains in Eq. (2), which corresponds to the differential cross section for the ZH production process.

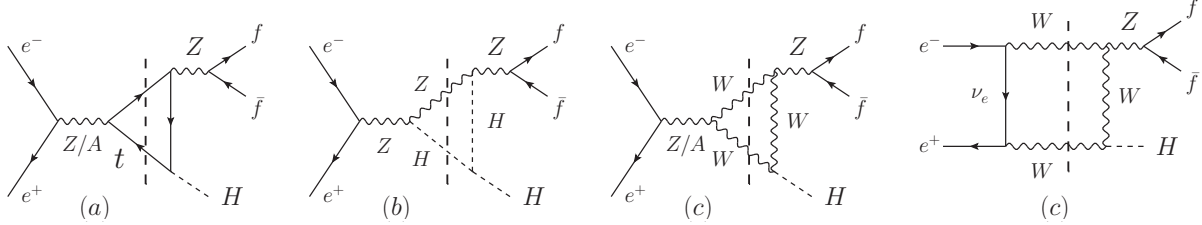


FIG. 2. Representative one-loop Feynman diagrams that contribute to the T-odd distribution, (a) the top loop diagrams, (b) the Higgs loop diagram that depends on the coupling λ_3 , and (c) a part of the gauge boson loop diagrams.

The first six coefficients ($F_1, F_2, F_3, F_4, F_5, F_6$) are T-even and the last three coefficients (F_7, F_8, F_9) are T-odd. The leading contribution to the six T-even coefficients is calculated from the tree diagram shown in Fig. 1. The amplitude for the production process can be in general written as

$$\mathcal{M}_\tau^\lambda = \bar{v}(\bar{p}, -\tau)\Gamma^\mu u(p, \tau)\epsilon_\mu^*(k, \lambda), \quad (3)$$

where u and v are the spinors for the electron and the positron, respectively, ϵ_μ the Z polarization vectors, λ the Z boson helicity, and p , \bar{p} and k are the four-momenta of the electron, positron and Z boson, respectively. The four-vector Γ_μ in the one-loop calculation can be expanded as

$$\Gamma_\mu = \sum_{\rho=\mp} (a_{(1)\rho}\gamma_\mu + a_{(2)\rho}p_\mu \not{k} + a_{(3)\rho}\bar{p}_\mu \not{k}) \frac{1 + \rho\gamma_5}{2}. \quad (4)$$

The six coefficients $a_{(i)\mp}$ ($i = 1$ to 3) are complex numbers, independent of τ and λ . In the tree-level calculation, only $a_{(1)\mp}$ are non-zero:

$$\begin{aligned} A_- &\equiv a_{(1)-}^{(\text{tree})} = (s - m_Z^2)^{-1} \frac{4\pi\alpha}{s_W^2 c_W^2} (-1/2 + s_W^2) m_Z, \\ A_+ &\equiv a_{(1)+}^{(\text{tree})} = (s - m_Z^2)^{-1} \frac{4\pi\alpha}{c_W^2} m_Z, \\ a_{(2)-}^{(\text{tree})} &= a_{(2)+}^{(\text{tree})} = a_{(3)-}^{(\text{tree})} = a_{(3)+}^{(\text{tree})} = 0, \end{aligned} \quad (5)$$

where $\alpha = e^2/(4\pi)$ with e being the magnitude of the electron charge, $c_W = \cos\theta_W$ and $s_W = \sin\theta_W$ are the weak mixing factors. We define the coordinate system of the Z rest frame as follows: the z axis is along the original Z momentum direction and the y axis is along the direction of $\vec{p} \times (-\vec{p})$. The tree-level prediction for the angular coefficients in our coordinate system is

$$F_i(\tau, \cos\Theta) = \frac{3|\vec{k}|}{256\pi^2 s^{3/2}} \sum_{f,\tau'} B_f \frac{(v_f + \tau' a_f)^2}{2(v_f^2 + a_f^2)} f_i(\tau, \tau', \cos\Theta) \quad (6)$$

with

$$\begin{aligned} f_1 &= A_\tau^2 s \left(1 + \cos^2\Theta + \frac{w^2}{m_Z^2} \sin^2\Theta \right), \\ f_2 &= A_\tau^2 s \frac{w^2}{m_Z^2} \sin^2\Theta, \\ f_3 &= -A_\tau^2 s \frac{w}{m_Z} \sin 2\Theta, \\ f_4 &= A_\tau^2 s \sin^2\Theta, \\ f_5 &= 4\tau\tau' A_\tau^2 s \cos\Theta, \\ f_6 &= -4\tau\tau' A_\tau^2 s \frac{w}{m_Z} \sin\Theta, \\ f_7 &= f_8 = f_9 = 0, \end{aligned} \quad (7)$$

where w is the Z boson energy $w = (s + m_Z^2 - m_H^2)/(2\sqrt{s})$, \vec{k} is the Z boson three momentum $|\vec{k}| = \sqrt{w^2 - m_Z^2}$, B_f is the branching fraction $B_f = \Gamma(Z \rightarrow f\bar{f})/\Gamma(Z \rightarrow \text{all})$, v_f and a_f are the vector and axial-vector couplings of the Z to the final fermion f , and τ' is the final fermion helicity. At the tree-level, the T-odd coefficients are vanishing as expected. The first non-vanishing contribution comes from the interference between the tree diagram and the absorptive part of the one-loop diagrams ⁴:

$$\begin{aligned} f_7 &= 2\tau' A_\tau \frac{s^{3/2}}{m_Z} |\vec{k}| \sin\Theta \left\{ w \text{Im} \left(a_{(2)\tau}^{(\text{loop})} - a_{(3)\tau}^{(\text{loop})} \right) - |\vec{k}| \cos\Theta \text{Im} \left(a_{(2)\tau}^{(\text{loop})} + a_{(3)\tau}^{(\text{loop})} \right) \right\}, \\ f_8 &= \tau A_\tau \frac{s^{3/2}}{m_Z} |\vec{k}| \sin\Theta \left\{ w \cos\Theta \text{Im} \left(a_{(2)\tau}^{(\text{loop})} - a_{(3)\tau}^{(\text{loop})} \right) - |\vec{k}| \text{Im} \left(a_{(2)\tau}^{(\text{loop})} + a_{(3)\tau}^{(\text{loop})} \right) \right\}, \\ f_9 &= -\tau A_\tau s^{3/2} |\vec{k}| \sin^2\Theta \text{Im} \left(a_{(2)\tau}^{(\text{loop})} - a_{(3)\tau}^{(\text{loop})} \right). \end{aligned} \quad (8)$$

⁴ Here the $Z \rightarrow f\bar{f}$ decay is always the tree level calculation. This is sufficient for our purpose, since the absorptive part of the one-loop diagrams in $Z \rightarrow f\bar{f}$ does not produce the T-odd distribution in the massless fermion limit.

Note that the absorptive part in this order is both ultraviolet and infrared finite. We notice that $\text{Im}(a_{(1)\mp}^{(\text{loop})})$ do not contribute to the T-odd coefficients. As a result, we need to calculate the absorptive part of only a limited one-loop diagrams, representatives of which are shown in Fig. 2. We divide the relevant one-loop diagrams into three categories, namely, top loop diagrams, a Higgs loop diagram that depends on the coupling λ_3 , and gauge boson loop diagrams. These are labeled as (a), (b) and (c), respectively, in Fig. 2. They are separately gauge-independent. The electroweak one-loop diagrams and amplitude are generated with help of `FeynArts` [38] and `FormCalc` [39]. The analytic formulas for $\text{Im}(a_{(2)\mp}^{(\text{loop})})$ and $\text{Im}(a_{(3)\mp}^{(\text{loop})})$ have been obtained but they are very long expressions and will be provided elsewhere [40]. The numerical values for the one-loop scalar functions are calculated with the `LoopTools` [39, 41]. Phase space integration is performed with `BASES` [42]. Our calculation has been numerically checked in the following two ways. First, CP invariance of the differential cross section [43, 44] has been tested. Second, the T-odd coefficients have been also calculated from the electroweak full one-loop helicity amplitudes using `MadGraph5_aMC@NLO` [45, 46]. We have found perfect agreement for several phase space points.

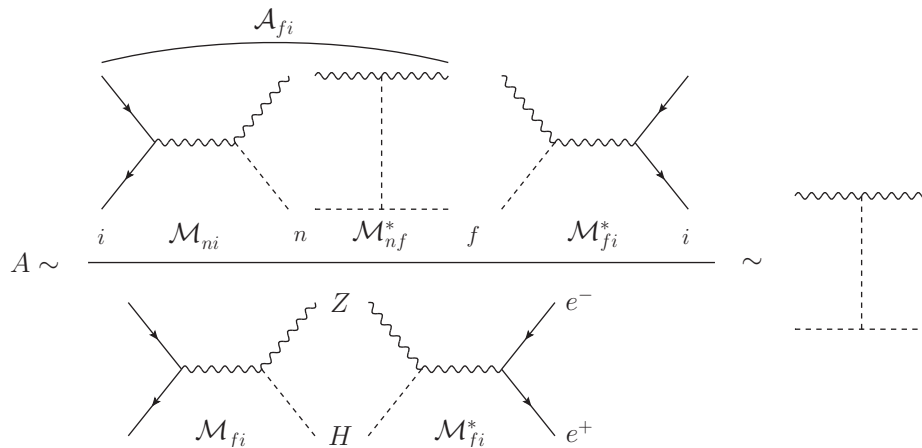


FIG. 3. Diagrams contributing to the numerator and denominator in the T-odd asymmetries in Eq. (9). \mathcal{A}_{fi} represents the absorptive part of the Higgs one-loop diagram. The asymmetries measure the tree-level t -channel $ZH \rightarrow ZH$ scattering.

The leading order prediction for T-odd asymmetries is of order $g^2/(4\pi)$ and can be obtained by dividing the T-odd coefficients (F_7, F_8, F_9) in Eq. (8) by the T-even coefficient F_1

in Eq. (7) . We define the integrated T-odd asymmetries by

$$\begin{aligned}
A_7 &\equiv \frac{\sum_{\tau} \xi(\tau) \left(\int_0^1 - \int_{-1}^0 \right) d \cos \Theta F_7(\tau, \cos \Theta)}{\sum_{\tau} \xi(\tau) \int_{-1}^1 d \cos \Theta F_1(\tau, \cos \Theta)}, \\
A_8 &\equiv \frac{\sum_{\tau} \xi(\tau) \int_{-1}^1 d \cos \Theta F_8(\tau, \cos \Theta)}{\sum_{\tau} \xi(\tau) \int_{-1}^1 d \cos \Theta F_1(\tau, \cos \Theta)},
\end{aligned} \tag{9}$$

where $\xi(\tau) = (1 + \tau P_{e^-})(1 - \tau P_{e^+})$ and, $1 \leq P_{e^-} (P_{e^+}) \leq 1$ denotes the degree of longitudinal polarization of the electron (positron) beam. The integration over $\cos \Theta$ takes into account the CP invariance of the differential cross section. We have found that the coefficient F_9 receives contribution only from the gauge boson loop diagrams (c) in Fig. 2 [40], therefore an asymmetry based on it is not useful for our purpose. In Fig. (3), diagrams contributing to the numerator and denominator in the T-odd asymmetries are described. Here \mathcal{A}_{fi} represents the absorptive part of only the Higgs one-loop diagram ⁵. It is shown that, because an absorptive part of one-loop amplitude is simply a tree amplitude times a tree amplitude, the tree diagram for $e^+e^- \rightarrow ZH$ drops from the ratio and only the tree diagram for the $ZH \rightarrow ZH$ scattering (t -channel) is left. This explains that the T-odd asymmetries measure the tree-level $ZH \rightarrow ZH$ scattering, and because the coupling λ_3 is no longer a part of the loop, the T-odd asymmetries are direct probes of λ_3 . The asymmetries depend also on the ZZH coupling. However, the ZZH coupling can be constrained separately via a precise measurement of the cross section. Therefore, we can use it as input to predict the asymmetries, focusing only on constraining deviation in λ_3 .

We use the following set of input parameters for the numerical results:

$$\begin{aligned}
m_H &= 125, \quad m_W = 80.419, \quad m_Z = 91.188, \quad m_t = 174.3, \\
v &= 246.218, \quad s_W^2 = 0.222, \quad \alpha = 1/132.507
\end{aligned}$$

in units of GeV for the mass parameters. In the following numerical studies, we restrict ourselves to the case $m_Z + m_H < \sqrt{s} < m_Z + 2m_H$, in which case the direct λ_3 measurement in $e^+e^- \rightarrow ZHH$ is not possible. Since the c.m. energy chosen is also below the $t\bar{t}$ threshold, i.e. $\sqrt{s} < 2m_t$, the top loop diagrams do not contribute to the T-odd asymmetries and we can avoid any ambiguity from a modified top Yukawa coupling due to a high scale NP, which is unavoidable in the indirect method [11]. We separate the contribution from the Higgs

⁵ The explicit formula of T-odd quantities in terms of an absorptive part can be found in Refs. [32, 33, 36].

loop diagram and that from the gauge boson loop diagrams to the SM asymmetries as,

$$A_i^{\text{SM}} = A_i^{\text{Higgs}} + A_i^{\text{Gauge}} \quad \text{for } i = 7, 8. \quad (10)$$

Observation of A_7 requires the charge identification of the final fermion f . This requirement is easily met for the decay modes $Z \rightarrow \ell^- \ell^+$. The charge of a B meson containing one b or \bar{b} quark can be identified via the decay mode $B \rightarrow \ell \nu + X$. We assume an efficiency of 20% for identifying the charges of the decaying b or \bar{b} hadrons [44]. The asymmetries receive unpleasant suppressions due to the fact that the T-odd coefficients are also parity-odd in case we do not measure the spin of the initial and final states [36]. Techniques to reduce the suppressions are as follows. The asymmetry A_7 vanishes if the $Z \rightarrow f \bar{f}$ decay process conserves parity. Since the coupling of the charged lepton to the Z is almost axial-vector, A_7 in the $Z \rightarrow e^- e^+$ and $Z \rightarrow \mu^- \mu^+$ decay modes has the suppression factor of $\sim 1/5$, which is unavoidable. However, for some fraction of the $Z \rightarrow \tau^- \tau^+$ decay, we can measure the τ helicity from τ decay distributions [47, 48] and reduce the suppression factor. We assume an efficiency of 40% for measuring the τ helicity [44]. Similarly, the asymmetry A_8 vanishes if parity is conserved in the production process, namely if $a_{(i)-} = a_{(i)+}$ for all $i = 1, 2, 3$. Due to the coupling of the incoming electron to the Z being dominantly axial-vector, the Higgs loop contribution A_8^{Higgs} is very suppressed without beam polarization. Fortunately, polarized beams can be available in future $e^- e^+$ colliders [6].

In Fig. 4, we display the variation of $(A_7^{\text{SM}}, A_8^{\text{SM}})$ and $(A_7^{\text{Higgs}}, A_8^{\text{Higgs}})$ as functions of the c.m. energy for two practical choices of beam polarizations: $(P_{e^-}, P_{e^+}) = (-0.80, +0.30)$, and $(+0.80, -0.30)$. We find that the absolute values of the asymmetries are small ($\lesssim 1\%$) and they grow as the beam energy is increased. For both the choices of beam polarizations, $(A_8^{\text{SM}}, A_8^{\text{Higgs}})$ are larger than $(A_7^{\text{SM}}, A_7^{\text{Higgs}})$, respectively. This indicates that A_8 can play a more important role than A_7 in bounding λ_3 . The Higgs loop contribution $(A_7^{\text{Higgs}}, A_8^{\text{Higgs}})$ to the asymmetries also become larger at higher c.m. energies, implying a higher sensitivity to λ_3 at a higher beam energy.

We parametrize the NP effect on the trilinear self-coupling in terms of a real parameter δ_h as

$$\lambda_3 = \lambda_3^{\text{SM}}(1 + \delta_h), \quad (11)$$

where, $\delta_h = 0$ gives the SM prediction for λ_3 . Because A_i^{Higgs} is proportional to λ_3 , the

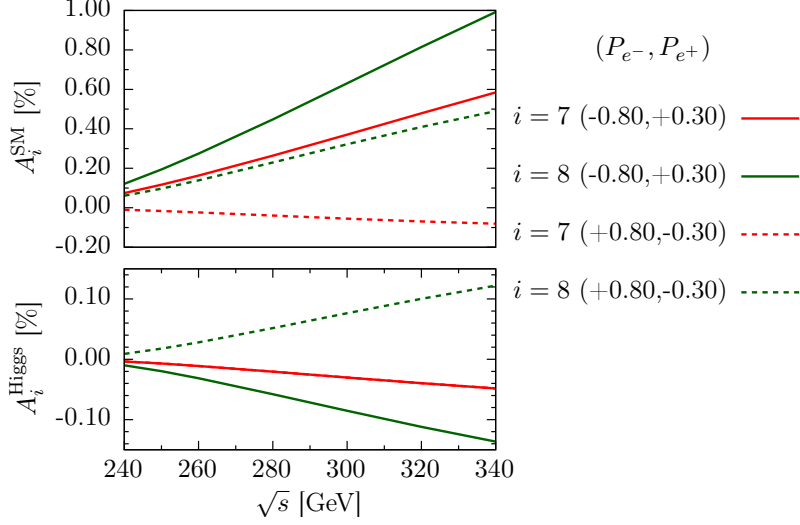


FIG. 4. ($A_7^{\text{SM}}, A_8^{\text{SM}}$) in the upper plot and ($A_7^{\text{Higgs}}, A_8^{\text{Higgs}}$) in the lower plot as functions of the c.m. energy, for two choices of beam polarizations: $(-0.80, +0.30)$ (solid) and $(+0.80, -0.30)$ (dashed). A_7^{Higgs} for the two choices of polarizations are degenerate.

asymmetries with nonzero δ_h can be described as

$$A_i^{\text{BSM}} = \delta_h \times A_i^{\text{Higgs}} + A_i^{\text{SM}} \quad \text{for } i = 7, 8. \quad (12)$$

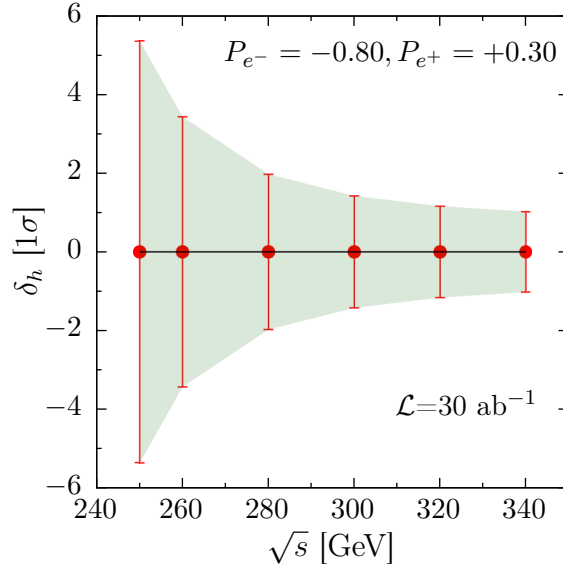


FIG. 5. Direct 1σ constraint on δ_h obtained from the T-odd asymmetries (A_7, A_8) at several c.m. energies, with beam polarization $(-0.80, +0.30)$ and an integrated luminosity of 30 ab^{-1} .

In Fig. 5, we provide direct 1σ bound on the SM value of δ_h that can be reached at different

c.m. energies by measuring the asymmetries (A_7, A_8) . The result is obtained for beam polarization of $(-0.80, +0.30)$ which provides better sensitivity due to a larger statistics and the larger asymmetry A_8^{Higgs} ; see Fig. 4. We have also assumed an integrated luminosity of 30 ab^{-1} . By definition, the asymmetries are less sensitive to systematic uncertainties, therefore, in our analysis, we consider only the statistical uncertainty. Despite a decrease in the total cross section with the rise of the beam energy, the constraint on δ_h improves and we can reach an accuracy of about 100% below the ZHH threshold. We have explicitly verified that the accuracy on λ_3 does not change appreciably if uncertainty on ZZH coupling is less than 10%. Since the asymmetries depend on δ_h linearly, the same level of accuracy can be achieved for non-SM values of the parameter δ_h as well.

To summarize, a direct measurement of the Higgs self-coupling λ_3 is possible even in the single Higgs production process $e^+e^- \rightarrow ZH$ by using the T-odd asymmetries. Due to the smallness of the asymmetries ($\lesssim 1\%$), the method is very challenging and requires a huge statistics. Our analysis with a beam polarization $(-0.80, +0.30)$ and an integrated luminosity of 30 ab^{-1} suggests that using this method we can measure λ_3 with an accuracy of $\sim 100\%$ at $\sqrt{s} = 340 \text{ GeV}$. However, the following benefits of the proposed method should be emphasized:

(1) Any ambiguity from a possible modification in the top Yukawa coupling is absent in a measured λ_3 , when the beam energy is below the $t\bar{t}$ threshold.

(2) Since the T-odd asymmetries are independent information from the ZH production cross section, the ZZH coupling which also contributes to the asymmetries can be very well constrained through the cross section measurement and, therefore, the asymmetries can be utilized to constrain λ_3 only.

(3) This is so far the only approach to directly measure λ_3 in e^+e^- collisions, when a beam energy above the ZHH threshold is not available.

ACKNOWLEDGMENTS

The authors wish to thank F. Maltoni and X. Zhao for reading the manuscript. The authors are grateful to J. Baglio, D. Gonçalves, K. Hagiwara, B. Jäger, F. Maltoni, L. D. Ninh and X. Zhao for fruitful discussions, and V. Hirschi and O. Mattelaer for their help

with `MadGraph5_aMC@NLO` package. J.N. would also like to thank K. Hagiwara for encouragement. J.N. would like to acknowledge the warm hospitality of the KEK Theory Center and CP3 Louvain, where he has carried out a part of the work. J.N. is also grateful for the support from MEXT KAKENHI Grant Number JP16K21730. J.N. very much appreciates the support from the Alexander von Humboldt Foundation. The work of A.S. is supported by MOVE- IN Louvain incoming postdoctoral fellowship co-funded by the Marie Curie Actions of the European Commission.

-
- [1] U. Baur, T. Plehn, and D. L. Rainwater, *Phys. Rev. Lett.* **89**, 151801 (2002), arXiv:hep-ph/0206024 [hep-ph].
 - [2] U. Baur, T. Plehn, and D. L. Rainwater, *Phys. Rev.* **D69**, 053004 (2004), arXiv:hep-ph/0310056 [hep-ph].
 - [3] U. Baur, *Phys. Rev.* **D80**, 013012 (2009), arXiv:0906.0028 [hep-ph].
 - [4] M. J. Dolan, C. Englert, and M. Spannowsky, *JHEP* **10**, 112 (2012), arXiv:1206.5001 [hep-ph].
 - [5] J. Baglio, A. Djouadi, R. Gröber, M. M. Mühlleitner, J. Quevillon, and M. Spira, *JHEP* **04**, 151 (2013), arXiv:1212.5581 [hep-ph].
 - [6] H. Baer, T. Barklow, K. Fujii, Y. Gao, A. Hoang, S. Kanemura, J. List, H. E. Logan, A. Nomerotski, M. Perelstein, *et al.*, (2013), arXiv:1306.6352 [hep-ph].
 - [7] D. M. Asner *et al.*, in *Proceedings, 2013 Community Summer Study on the Future of U.S. Particle Physics: Snowmass on the Mississippi (CSS2013): Minneapolis, MN, USA, July 29-August 6, 2013* (2013) arXiv:1310.0763 [hep-ph].
 - [8] M. McCullough, *Phys. Rev.* **D90**, 015001 (2014), [Erratum: *Phys. Rev.* **D92**, no.3, 039903(2015)], arXiv:1312.3322 [hep-ph].
 - [9] R. Frederix, S. Frixione, V. Hirschi, F. Maltoni, O. Mattelaer, P. Torrielli, E. Vryonidou, and M. Zaro, *Phys. Lett.* **B732**, 142 (2014), arXiv:1401.7340 [hep-ph].
 - [10] A. Azatov, R. Contino, G. Panico, and M. Son, *Phys. Rev.* **D92**, 035001 (2015), arXiv:1502.00539 [hep-ph].
 - [11] C. Shen and S.-h. Zhu, *Phys. Rev.* **D92**, 094001 (2015), arXiv:1504.05626 [hep-ph].
 - [12] M. Gorbahn and U. Haisch, *JHEP* **10**, 094 (2016), arXiv:1607.03773 [hep-ph].
 - [13] G. Degrandi, P. P. Giardino, F. Maltoni, and D. Pagani, *JHEP* **12**, 080 (2016),

- arXiv:1607.04251 [hep-ph].
- [14] W. Bizon, M. Gorbahn, U. Haisch, and G. Zanderighi, *JHEP* **07**, 083 (2017), arXiv:1610.05771 [hep-ph].
- [15] F. Bishara, R. Contino, and J. Rojo, *Eur. Phys. J.* **C77**, 481 (2017), arXiv:1611.03860 [hep-ph].
- [16] S. Di Vita, C. Grojean, G. Panico, M. Riembau, and T. Vantalon, *JHEP* **09**, 069 (2017), arXiv:1704.01953 [hep-ph].
- [17] S. Di Vita, G. Durieux, C. Grojean, J. Gu, Z. Liu, G. Panico, M. Riembau, and T. Vantalon, *JHEP* **02**, 178 (2018), arXiv:1711.03978 [hep-ph].
- [18] F. Maltoni, D. Pagani, A. Shivaji, and X. Zhao, *Eur. Phys. J.* **C77**, 887 (2017), arXiv:1709.08649 [hep-ph].
- [19] *Study of the double Higgs production channel $H(\rightarrow b\bar{b})H(\rightarrow \gamma\gamma)$ with the ATLAS experiment at the HL-LHC*, Tech. Rep. ATL-PHYS-PUB-2017-001 (CERN, Geneva, 2017).
- [20] *Combination of searches for Higgs boson pair production in proton-proton collisions at $\sqrt{s} = 13$ TeV*, Tech. Rep. CMS-PAS-HIG-17-030 (CERN, Geneva, 2018).
- [21] D. Gonçalves, T. Han, F. Kling, T. Plehn, and M. Takeuchi, *Phys. Rev.* **D97**, 113004 (2018), arXiv:1802.04319 [hep-ph].
- [22] F. Maltoni, D. Pagani, and X. Zhao, *JHEP* **07**, 087 (2018), arXiv:1802.07616 [hep-ph].
- [23] S. D. Rindani and B. Singh, (2018), arXiv:1805.03417 [hep-ph].
- [24] *Combination of searches for Higgs boson pairs in pp collisions at 13 TeV with the ATLAS experiment.*, Tech. Rep. ATLAS-CONF-2018-043 (CERN, Geneva, 2018).
- [25] W. Bizoń, U. Haisch, and L. Rottoli, (2018), arXiv:1810.04665 [hep-ph].
- [26] S. Borowka, C. Duhr, F. Maltoni, D. Pagani, A. Shivaji, and X. Zhao, (2018), arXiv:1811.12366 [hep-ph].
- [27] *Constraints on the Higgs boson self-coupling from $t\bar{t}H+tH$, H to gamma gamma differential measurements at the HL-LHC*, Tech. Rep. CMS-PAS-FTR-18-020 (CERN, Geneva, 2018).
- [28] J. Fleischer and F. Jegerlehner, *Nucl. Phys.* **B216**, 469 (1983).
- [29] J. Fleischer and F. Jegerlehner, *Nucl. Phys.* **B228**, 1 (1983).
- [30] S. Dawson and H. E. Haber, *Phys. Rev.* **D44**, 53 (1991).
- [31] B. A. Kniehl, *Z. Phys.* **C55**, 605 (1992).
- [32] A. De Rujula, J. M. Kaplan, and E. De Rafael, *Nucl. Phys.* **B35**, 365 (1971).

- [33] A. De Rujula, R. Petronzio, and B. E. Lautrup, Nucl. Phys. **B146**, 50 (1978).
- [34] K. Fabricius, I. Schmitt, G. Kramer, and G. Schierholz, Phys. Rev. Lett. **45**, 867 (1980).
- [35] K. Hagiwara, K.-i. Hikasa, and N. Kai, Phys. Rev. Lett. **47**, 983 (1981).
- [36] K. Hagiwara, K.-i. Hikasa, and N. Kai, Phys. Rev. **D27**, 84 (1983).
- [37] K.-i. Hikasa, Phys. Lett. **128B**, 253 (1983).
- [38] T. Hahn, Comput. Phys. Commun. **140**, 418 (2001), arXiv:hep-ph/0012260 [hep-ph].
- [39] T. Hahn and M. Perez-Victoria, Comput. Phys. Commun. **118**, 153 (1999), arXiv:hep-ph/9807565 [hep-ph].
- [40] J. Nakamura and A. Shivaji, To be published.
- [41] G. J. van Oldenborgh and J. A. M. Vermaseren, Z. Phys. **C46**, 425 (1990).
- [42] S. Kawabata, Comput. Phys. Commun. **88**, 309 (1995).
- [43] K. Hagiwara and M. L. Stong, Z. Phys. **C62**, 99 (1994), arXiv:hep-ph/9309248 [hep-ph].
- [44] K. Hagiwara, S. Ishihara, J. Kamoshita, and B. A. Kniehl, Eur. Phys. J. **C14**, 457 (2000), arXiv:hep-ph/0002043 [hep-ph].
- [45] J. Alwall, R. Frederix, S. Frixione, V. Hirschi, F. Maltoni, O. Mattelaer, H. S. Shao, T. Stelzer, P. Torrielli, and M. Zaro, JHEP **07**, 079 (2014), arXiv:1405.0301 [hep-ph].
- [46] R. Frederix, S. Frixione, V. Hirschi, D. Pagani, H. S. Shao, and M. Zaro, JHEP **07**, 185 (2018), arXiv:1804.10017 [hep-ph].
- [47] B. K. Bullock, K. Hagiwara, and A. D. Martin, Nucl. Phys. **B395**, 499 (1993).
- [48] K. Hagiwara, T. Li, K. Mawatari, and J. Nakamura, Eur. Phys. J. **C73**, 2489 (2013), arXiv:1212.6247 [hep-ph].